https://doi.org/10.5194/acp-2020-597
Preprint. Discussion started: 14 July 2020

Atmospheric Chemistry and Physics Discussions

Insights into particulate matter pollution in the North China Plain during wintertime: Local contribution or regional transport?

Jiarui Wu[1,4], Naifang Bei[2], Yuan Wang[3], Xia Li[1,4], Suixin Liu[1,4], Lang Liu[1,4], Ruonan Wang[1,4], Jiaoyang Yu[1], Min Zuo[1,4], Zhenxing Shen[2], Junji Cao[1,4], Xuexi Tie[1], and Guohui Li[1,4*]

[1]Key Lab of Aerosol Chemistry and Physics, SKLLQG, Institute of Earth Environment, Chinese Academy of Sciences, Xi'an, 710061, China
[2]School of Human Settlements and Civil Engineering, Xi'an Jiaotong University, Xi'an, 710049, China
[3]Division of Geological and Planetary Sciences, California Institute of Technology, Pasadena, CA 91125, USA
[4]CAS Center for Excellence in Quaternary Science and Global Change, Xi'an, 710061, China

[*]Correspondence to: Guohui Li (ligh@ieecas.cn)

Abstract. Accurate identification and quantitative source apportionment of fine particulate matters ($PM_{2.5}$) provide an important prerequisite for design and implementation of emission control strategies to reduce PM pollution. Therefore, a source-oriented version of the WRF-Chem model is developed in the study to make source apportionment of $PM_{2.5}$ in the North China Plain (NCP). A persistent and heavy haze event occurred in the NCP from 05 December 2015 to 04 January 2016 is simulated using the model as a case study to quantify $PM_{2.5}$ contributions of local emissions and regional transport. Results show that local and non-local emissions contribute 36.3% and 63.7% of the $PM_{2.5}$ mass in Beijing during the haze event on average. When Beijing's air quality is excellent or good in terms of hourly $PM_{2.5}$ concentrations, local emissions dominate the $PM_{2.5}$ mass with contributions exceeding 50%. However, when the air quality is severely polluted, the $PM_{2.5}$ contribution of non-local emissions is around 75%. The non-local emissions also dominate the Tianjin's air quality, with average $PM_{2.5}$ contributions exceeding 70%. The $PM_{2.5}$ level in Hebei and Shandong is generally controlled by local emissions, but in Henan, local and non-local emissions play an almost equivalent role in the $PM_{2.5}$ level, except when the air quality is severely polluted, with non-local $PM_{2.5}$ contributions of over 60%. Additionally, the primary aerosol species are generally dominated by local emissions with the average contribution exceeding 50%. However, the source apportionment of secondary aerosols shows more evident regional characteristics. Therefore, except cooperation with neighboring provinces to carry out strict emission mitigation measures, reducing primary aerosols constitutes the priority to alleviate PM pollution in the NCP, especially in Beijing and Tianjin.

https://doi.org/10.5194/acp-2020-597
Preprint. Discussion started: 14 July 2020

1 Introduction

As the most polluted area in China, the North China Plain (NCP) has been suffering severe particulate pollution for recent decades, particularly during wintertime, caused by a synergy of local emissions, trans-boundary transport, specific topography, and unfavorable meteorological situations (Long et al., 2016; Wu et al., 2017; An et al., 2019; Wu et al., 2020). In recent years, China government has carried out aggressive emission mitigation measures to reduce particulate matter (PM) pollution (Zheng et al., 2018; Zhang et al., 2019), but heavy haze with high $PM_{2.5}$ (fine PM) concentrations still frequently engulfs the area. It is controversial on whether local emissions or trans-boundary transport dominates the PM pollution in the NCP, especially in Beijing (Guo et al., 2014; Li et al., 2015; Zhang et al., 2015; Wu et al., 2017; Zamora et al., 2019). Therefore, accurate identification and quantitative source apportionment (SA) of $PM_{2.5}$ are imperative to provide scientific reference for instituting air quality control strategies as well as constitute an important prerequisite to reduce PM pollution in the NCP.

The observation based SA techniques, such as chemical mass balance (CMB) and positive matrix factorization (PMF) methods, are traditionally used to quantify the particle contribution of each source (Cooper and Watson, 1980; Paatero and Tapper, 1993), but cannot identify the source contribution of secondary transformation to particulate matters. The brute force method (BFM) is the simplest model based SA method using air quality models (AQMs) through zeroing out emissions from a specific source (Marmur et al., 2005). The BFM can assess the importance of each emission source, but has flaws in quantifying the source contribution due to lack of consideration of the complicated non-linear interaction between various sources (Zhang and Ying, 2011). At present, the widely used SA technique based on AQMs is the reactive tracer method or the source-oriented AQMs (Marmur et al., 2006; Ying and Kleeman, 2006; Ying et al., 2008a; Ying et al., 2008b; Zhang and Ying, 2010,

https://doi.org/10.5194/acp-2020-597
Preprint. Discussion started: 14 July 2020

2011; Burr and Zhang, 2011; Zhang et al., 2014). The method adds reactive tracers or tagged species in AQMs to trace the atmospheric transport, transformation, and deposition of air pollutants emitted from specific sources and quantify the source contribution according to the mass conservation (Wagstrom et al., 2008; Wang et al., 2009).

The observation based SA method or the BFM based on AQMs has been used to evaluate $PM_{2.5}$ contributions of local emissions and trans-boundary transport in the NCP, especially in Beijing-Tianjin-Hebei (BTH). Chang et al. (2019) have investigated the contribution of trans-boundary transport to the $PM_{2.5}$ concentration in 13 cities of the BTH, showing that Shandong province has a considerable $PM_{2.5}$ contribution to most cities in BTH, followed by Henan among the four neighboring provinces. Dong et al. (2020) have also found that the regional transport contributes about 32.5%-68.4% of $PM_{2.5}$ concentrations in BTH in 2017. However, the contribution of local emissions or trans-boundary transport to Beijing's PM pollution still remains uncertain. Lang et al. (2013) have indicated that regional transport accounts for 54.6% of $PM_{2.5}$ concentrations during the polluted episode in Beijing, with annual $PM_{2.5}$ contribution of 42.4% on average using the observation and MM5–CMAQ model results. Wu et al. (2017) have shown that non-Beijing emissions contribute 61.5% of $PM_{2.5}$ mass during haze events in summer. However, some studies have emphasized that the severe haze formation occurred in Beijing is mainly controlled by the efficient local aerosol nucleation and growth, whereas the $PM_{2.5}$ contribution of regional transport might not be significant (Guo et al., 2014; Zamora et al., 2019). Meng et al. (2020) found that the regional transport from Hebei and Shandong plays an important role in the PM pollution in Tianjin, with the average $PM_{2.5}$ contribution of 44% during the wintertime, but the local contribution gradually dominates with continuous deterioration of the PM pollution. Wang et al. (2015) have concluded that regional transport plays a non-negligible role in the top three polluted cities in Hebei using the BFM method, with $PM_{2.5}$ contributions of 27.9% in Shijiazhuang,

https://doi.org/10.5194/acp-2020-597
Preprint. Discussion started: 14 July 2020

46.6% in Xingtai, and 40.4% in Handan. However, Wang et al. (2019) have proposed that local emissions are the main contributor to the air pollution in Hebei. Liu et al. (2017) have emphasized that the contribution of regional transport to the PM pollution in Henan is significant during the wintertime, with the average $PM_{2.5}$ contribution of 11.95%, 11.69%, 7.95%, and 7.4% from BTH, Anhui, Jiangsu, and Shandong, respectively. It is obvious that whether local contribution or regional transport is dominant during the PM pollution in the NCP is still uncertain.

In the study, a source-oriented WRF-Chem model is developed to comprehensively quantify the contribution of local emissions and trans-boundary transport to the PM pollution in the NCP, including Beijing, Tianjin, Hebei, Henan, and Shandong, as well as the adjacent province on the west, Shanxi, under different pollution levels during the wintertime in 2015.

2 Model and methodology

2.1 WRF-Chem model and configurations

The source-oriented AQM used in the study is based on the WRF-Chem model (Version 3.5) (Grell et al., 2005) with modifications by Li et al. (2010, 2011a, 2011b). The modified WRF-Chem model includes a new flexible gas phase chemical module that can be used with different chemical mechanisms and the CMAQ aerosol module (AERO5) developed by US EPA (Binkowski and Roselle, 2003; Foley et al., 2010). The wet deposition is based on the method in the CMAQ module and the dry deposition of chemical species follows Wesely (1989). The photolysis rates are calculated using the Fast Tropospheric Ultraviolet and Visible (FTUV) Radiation Model with the aerosol and cloud effects on photolysis (Li et al., 2005; Li et al., 2011a). The inorganic aerosols are predicted using ISORROPIA Version 1.7, calculating the composition and phase state of an ammonium-sulfate-nitrate-water inorganic aerosol in thermodynamic equilibrium with gas phase precursors (Nenes et al., 1998). The

https://doi.org/10.5194/acp-2020-597
Preprint. Discussion started: 14 July 2020

secondary organic aerosols (SOA) are calculated using the volatility basis-set (VBS) modeling method, with contributions from glyoxal and methylglyoxal. Detailed information can be found in Li et al. (2010, 2011a, 2011b). Figure 1 shows the simulation domain and detailed model configuration can be found in Table 1.

2.2 Source-Oriented WRF-Chem model

In the source-oriented WRF-Chem model, the SAPRC-99 photochemistry mechanism (Carter, 2010) and CMAQ aerosol module (AERO5) (Foley et al., 2010) are modified so that the precursors of aerosols from different sources and their corresponding reaction products are treated as different species and tracked independently in chemical, physical, and dynamic processes. It is worth noting that the tagged species have exactly identical physical and chemical properties as the original ones.

Black carbon and unspecified species (mainly mineral dust) from each source are tagged and only tracked in processes of transport, dispersion, and wet/dry deposition since they do not involve in photochemistry and gas-to-particle partitioning. For the inorganic aerosols (sulfate, nitrate, and ammonium) and organic aerosols (primary and secondary organic aerosols, i.e., POA and SOA), their precursors from each source and corresponding reaction products are treated as different species and simulated in the SAPRC-99 photochemistry mechanism and traced in processes of transport, dispersion, and wet/dry deposition as well as gas-to-particle partitioning. A non-hardwired gas phase chemical module is used to solve the SAPRC-99 photochemistry based on the Eulerian backward Gauss-Seidel iterative technique (Hess et al., 2000; Li et al., 2010). The module is flexible to include a new gas-phase species and its corresponding photochemical reactions.

The ISORROPIA is used to distribute the NH_3/ammonium, HNO_3/nitrate, and water between the gas and aerosol phases as a function of total sulfate, total ammonia, total nitrate, relative humidity and temperature (Nenes et al., 1998). Therefore, as a bulk method, the

https://doi.org/10.5194/acp-2020-597
Preprint. Discussion started: 14 July 2020

ISORROPIA cannot be applied to distribute the gas and aerosol phase for the inorganic aerosol from each source separately because of the interaction among various sources.

Except primary emissions, the SA for sulfate aerosols needs to be considered in the homogenous and heterogeneous formation pathways. The sulfate growth from the gas-phase SO_2 oxidation is contributed by the H_2SO_4 involved nucleation and condensation, which are determined by the H_2SO_4 formation rate in the atmosphere. At time $(\boldsymbol{t})$, after one time step $(\boldsymbol{\delta t})$ integeration, the conceptual scheme of the source-oriented sulfate gas-phase formation is shown in Figure 2a. In the study, the heterogeneous conversion of SO_2 is parameterized as the SO_2 oxidation involving aerosol water by O_2 catalyzed by $\boldsymbol{Fe^{3+}}$. Figure 2b presents the sulfate SA for the heterogeneous formation. The SA for nitrate and ammonium aerosols follows the mass conversion of $\boldsymbol{N(+VI)}$ and $\boldsymbol{N(-III)}$ from each source, respectively, when the total ammonia and nitrate are distributed between the gas and aerosol phases by the ISORROPIA after one time step integration, as shown in Figure 3.

Organic aerosols are simulated using a non-traditional SOA module based on the volatility basis set (VBS) method, in which all primary species are treated as chemically reactive and distributed in logarithmically spaced volatility bins (Donahue et al., 2006; Robinson et al., 2007). Nine surrogate species with saturation concentration ranging from 10^{-2} to 10^{6} μg m^{-3} at room temperature are considered to represent POA compositions (Shrivastava et al., 2008). The SOA formation from anthropogenic or biogenic precursors is predicted using four semi-volatile organic compounds (SVOCs) whose effective saturation concentrations at room temperature are 1, 10, 100, and 1000 μg m^{-3}, respectively (Tsimpidi et al., 2010). The SOA formation includes the following pathways: (1) the oxidation of VOCs emitted from anthropogenic and biogenic sources, (2) intermediate VOCs (IVOCs) co-emitted with POA but are never in the particle phase during the emissions process oxidized by OH, and (3) primary organic gases (POG) emitted or formed due to evaporation

https://doi.org/10.5194/acp-2020-597
Preprint. Discussion started: 14 July 2020

of POA assumed to react with OH radicals to reduce their volatility and hence to partition between gas and particle phase forming SOA (Odum et al., 1996; Pankow, 1994; Lipsky and Robinson, 2006; Robinson et al., 2007; Shrivastava et al., 2006). The VBS method is in principle source-oriented, which can be used to trace the OA formation from various sources. Therefore, when considering SA for organic aerosols, we just need to treat all the SOA and POA as well as their corresponding gas-phase organics from each emission source as the VBS input, as shown in Figure 4a. For the heterogeneous pathway, the SOA formation from glyoxal and methyglyoxal is parameterized as a first-order irreversible uptake on aerosol or cloud droplet surfaces with a reactive uptake coefficient of 3.7×10^{-3} (Volkamer et al., 2007; Zhao et al., 2006). The SA for heterogeneous SOA formation is shown in Figure 4b, which is similar to that for heterogeneous sulfate formation.

2.3 Data and statistical methods for comparisons

The model performance in simulating $PM_{2.5}$, O_3, NO_2, SO_2, and CO is validated using the hourly observations released by Ministry of Ecology and Environment of China (China MEP). In addition, the predicted submicron sulfate, nitrate, ammonium, and organic aerosols are compared to measurements by the Aerodyne Aerosol Chemical Speciation Monitor (ACSM), which is deployed at the National Center for Nanoscience and Technology (NCNST), Chinese Academy of Sciences in Beijing (Figure 1). The primary organic aerosol (POA) and SOA concentrations are obtained from the ACSM measurement analyzed using the positive matrix factorization (PMF).

In the present study, the mean bias (*MB*), root mean square error (*RMSE*) and the index of agreement (*IOA*) are used as indicators to evaluate the performance of WRF-Chem model. *IOA* describes the relative difference between the model and observation, ranging from 0 to 1, with 1 indicating perfect agreement.

$$\boldsymbol{MB} = \frac{1}{N}\sum_{i=1}^{N}(\boldsymbol{P_i} - \boldsymbol{O_i})$$

https://doi.org/10.5194/acp-2020-597
Preprint. Discussion started: 14 July 2020

$$\boldsymbol{RMSE} = \left[\frac{1}{N}\sum_{i=1}^{N}(\boldsymbol{P_i} - \boldsymbol{O_i})^2\right]^{\frac{1}{2}}$$

$$\boldsymbol{IOA} = 1 - \frac{\sum_{i=1}^{N}(\boldsymbol{P_i}-\boldsymbol{O_i})^2}{\sum_{i=1}^{N}(|\boldsymbol{P_i}-\overline{\boldsymbol{O}}|+|\boldsymbol{O_i}-\overline{\boldsymbol{O}}|)^2}$$

Where $\boldsymbol{P_i}$ and $\boldsymbol{O_i}$ are the predicted and observed pollutant concentrations, respectively. *N* is the total number of the predictions used for comparisons, and $\overline{\boldsymbol{P}}$ and $\overline{\boldsymbol{O}}$ represents the average of the prediction and observation, respectively.

3 Results and discussions

3.1 Model performance

Figure 5 shows the diurnal profiles of observed and simulated near-surface $PM_{2.5}$, O_3, NO_2, SO_2 and CO concentrations averaged at monitoring sites in the NCP from 05 December 2015 to 04 January 2016. The model generally performs well in reproducing the temporal variation of $PM_{2.5}$ concentrations in the NCP, with an *IOA* of 0.96, but slightly overestimates $PM_{2.5}$ concentrations against measurements, with a *MB* of 2.2 μg m^{-3}. The diurnal O_3 variation is successfully replicated by the model, such as peak afternoon O_3 concentrations caused by active photochemistry and low nighttime O_3 concentrations due to the NO_x titration, with an *IOA* of 0.88. However, the model is subject to underestimating the O_3 concentration compared to measurements, particularly during nighttime, with a *MB* of -5.9 μg m^{-3}. The model also reasonably well reproduces the NO_2 diurnal profiles with peaks in the evening, with an *IOA* of 0.89 and a *MB* of 0.5 μg m^{-3}, but considerable overestimations or underestimations still exist. The model generally tracks reasonably the temporal variation of SO_2 concentrations against observations, with an *IOA* of 0.76. However, the biases for the SO_2 simulation are also large considering that SO_2 is mainly emitted from point sources and its simulations are more sensitive to the wind field uncertainties (Bei et al., 2017). Compared with measurements, the temporal profile of the near-surface CO concentration in the NCP is

https://doi.org/10.5194/acp-2020-597
Preprint. Discussion started: 14 July 2020

well simulated, with the *IOA* and *MB* of 0.90 and 0.0 μg m^{-3}, respectively.

Figure 6 shows the spatial pattern of simulated and observed average near-surface concentrations of $PM_{2.5}$, O_3, NO_2, and SO_2 along with simulated winds during the episode in the NCP. The simulated air pollutants distributions are generally in good agreement with observations, although the model biases still exist. During the haze episode, the simulated weak or calm winds are favorable for accumulation of air pollutants, leading to formation of the serious air pollution in the NCP. The simulated average near-surface $PM_{2.5}$ concentrations during the episode are more than 115 μg m^{-3} in the NCP, which is consistent with observations. The simulated and observed average O_3 concentrations during the episode are not high, generally less than 40 μg m^{-3}. The low O_3 concentration during the episode is chiefly caused by the slow photochemical activities due to weak wintertime insolation which is further attenuated by clouds and aerosols and the resultant titration of high NO_x emissions (Li et al., 2018). The observed and calculated average NO_2 and SO_2 concentrations are still high in the NCP, varying from 30 to 100 μg m^{-3} and 20 to 100 μg m^{-3}, respectively, although strict emission mitigation measures have been carried out since 2013. Interestingly, the simulated SO_2 concentrations in cities and their surrounding areas are very high, but the simulated NO_2 concentrations present uniform distribution in the NCP, indicating the substantial contribution of NO_x area sources.

Figure 7 provides the temporal variations of simulated and observed aerosol species at NCNST in Beijing during the episode. Generally, the model predicts reasonably the temporal variations of the aerosol species against the measurements. The model yields the major peaks of the POA concentration compared to observations in Beijing, but frequently underestimates or overestimates the POA concentration, with an *IOA* of 0.80 and a *MB* of -2.0 μg m^{-3}. As a primary species, the POA in Beijing is determined by local emissions and regional transport outside of Beijing during haze days, so uncertainties from emissions and meteorological

https://doi.org/10.5194/acp-2020-597
Preprint. Discussion started: 14 July 2020

fields have large potential to influence POA simulations (Bei et al., 2017). Although the VBS modeling method is used and contributions from glyoxal and methylglyoxal are included in the study, the model still has difficulties in simulating the SOA concentrations, with the *IOA* and *MB* of 0.67 and -10.5 μg m^{-3}, respectively. Except the SOA formation and transformation mechanism in the atmosphere, which remains elusive, many factors have potentials to affect the SOA simulation, such as meteorology, measurements, precursor emissions, and SOA treatments (Li et al., 2011). The model reasonably reproduces the sulfate temporal variation compared to measurements, and the *MB* and *IOA* are -3.5 μg m^{-3} and 0.87, respectively. The model also performs well in simulating the nitrate and ammonium concentrations against measurements in Beijing, with *IOAs* of 0.92 and 0.88, respectively.

Generally, the model simulates well the spatial distribution and temporal variation of air pollutants in the NCP, and the predicted aerosol species are also consistent well with the measurements in Beijing. Good model performance in simulating air pollutants and aerosol species provides a reliable base for quantifying contributions of local and non-local emissions to the PM pollution in the NCP.

3.2 Source apportionment of the PM pollution in the NCP

We have marked the emitted precursors in six provinces, including Beijing, Tianjin, Hebei, Henan, Shandong, and Shanxi in simulations of the source-oriented WRF-Chem model (Figure 1). Additionally, the boundary transport and emissions from the region except the six provinces are taken as the background source. Therefore, $PM_{2.5}$ contributions of the non-local emission for each of the six provinces include those transported from the other five provinces and the background source.

Figure 8 shows the average $PM_{2.5}$ contribution of emissions from the six provinces during the study episode. Apparently, emissions from the six provinces influence the $PM_{2.5}$ level in the whole NCP, showing necessity of collaborative emission mitigation to reduce PM

https://doi.org/10.5194/acp-2020-597
Preprint. Discussion started: 14 July 2020

pollution. Emissions of Hebei, Henan, and Shandong not only significantly deteriorate the local PM pollution, with $PM_{2.5}$ contributions ranging from 50 to over 100 μg m^{-3}, also considerably enhance the $PM_{2.5}$ level in their surrounding areas by about 5~50 μg m^{-3}. Emissions of Beijing and Tianjin increase the local $PM_{2.5}$ concentrations by 10~100 μg m^{-3}, and contribute about 3~10 μg m^{-3} $PM_{2.5}$ to their surrounding areas. Due to blocking of mountains, $PM_{2.5}$ contributions of the Shanxi emission to the NCP is not significant, ranging from 3 to 20 μg m^{-3}.

Beijing is surrounded from the southwest to the northeast by the Taihang Mountains and the Yanshan Mountains and open to the NCP in the south and east. During haze events, southerly or easterly winds are generally prevailed in the NCP, facilitating transport of air pollutants emitted from the NCP to Beijing and further accumulation due to the mountain blocking (Long et al., 2016). During the study episode, the average simulated $PM_{2.5}$ concentration in Beijing is around 125.3 μg m^{-3}, in which the contribution of local emissions is 36.3%. The remaining 63.7% of $PM_{2.5}$ concentrations in Beijing is accounted for by non-Beijing emissions, showing that Beijing's air quality is dominated by non-Beijing emissions during the PM pollution episode. The $PM_{2.5}$ contribution of Hebei emissions to Beijing is 24.6%, greater than those of Shandong (8.3%), Tianjin (7.4%), Henan (3.6%), and Shanxi (3.3%). The background source contributes about 16.5% of the $PM_{2.5}$ mass in Beijing on average. Overall, the contribution of emissions from Beijing's five surrounding provinces to the $PM_{2.5}$ mass is 47.2%, exceeding that of local emissions, indicating the importance of the trans-boundary transport of air pollutants in the haze formation in Beijing. Adjacent to Beijing, the Tianjin's air quality is also dominated by trans-boundary transport of air pollutants. The average $PM_{2.5}$ contribution of non-local emissions is 76.2%, in which Hebei, Shandong, Beijing, Henan, and Shanxi accounts for 29.3%, 11.7%, 8.0%, 4.0%, and 3.0%, respectively. The $PM_{2.5}$ contribution of local emissions in Hebei, Henan, and Shanxi is

https://doi.org/10.5194/acp-2020-597
Preprint. Discussion started: 14 July 2020

almost as much as that of trans-boundary transport, with the average of 50.2%, 45.7%, and 49.2%, respectively. The Shandong emissions play an important role in the air quality in Hebei and Henan, with $PM_{2.5}$ contributions of about 15%. Moreover, the Shandong's air quality is primarily determined by emissions of itself, with an average $PM_{2.5}$ contribution of 64.9%. Emissions of Beijing, Tianjin, Hebei, Henan, and Shanxi contribute less than 8% of the $PM_{2.5}$ mass in Shandong. The background source makes up approximately 20.1%, 11.4%, 16.8%, 11.4%, and 21.8% of the $PM_{2.5}$ mass in Tianjin, Hebei, Henan, Shandong, and Shanxi, respectively.

Previous studies have shown that there exist large uncertainties on the contribution of local emissions or trans-boundary transport to Beijing's PM pollution (Guo et al., 2010; Guo et al., 2014; Li et al., 2015; Zhang et al., 2015; Wu et al., 2017). We further evaluate the contribution of local and non-local emissions to the $PM_{2.5}$ mass in Beijing under different pollution levels, as well as in the other five provinces. The simulated hourly near-surface $PM_{2.5}$ mass concentrations in Beijing during the whole episode are first subdivided into 6 bins based on the air quality standard in China for $PM_{2.5}$, i.e., 0~35 (excellent), 35~75 (good), 75~115 (lightly polluted), 115~150 (moderately polluted), 150~250 (heavily polluted), and exceeding 250 (severely polluted) μg m^{-3} (Feng et al., 2016). $PM_{2.5}$ contributions from local emissions and the other five provinces as well as background source to Beijing are assembled separately as the bin $PM_{2.5}$ concentrations following the grid cells, and an average of $PM_{2.5}$ contributions from each source in each bin is calculated. The same method is also used for the other five provinces.

Table 2, Table 3 and Figure 9 present the average percentage contribution of local and non-local emissions to the $PM_{2.5}$ concentrations in Beijing, Tianjin, Hebei, Henan, Shandong, and Shanxi during the episode under different pollution levels. The local emission dominates the $PM_{2.5}$ mass when the air quality is excellent and good in Beijing, with the average

https://doi.org/10.5194/acp-2020-597
Preprint. Discussion started: 14 July 2020

contribution of 56.8% and 55.0%, respectively. Moreover, the $PM_{2.5}$ contribution of local emissions decreases with the deterioration of the air quality in Beijing, with an average contribution of 48.7%, 40.5%, 35.4%, and 25.1%, respectively, when the air quality is slightly, moderately, heavily, and severely polluted. Therefore, non-local emissions play a dominant role in Beijing's PM pollution, particularly when the air quality is severely polluted, non-local emissions contribute around 75% of the $PM_{2.5}$ mass in Beijing. With the excellent and good air quality in Beijing, the contribution of emissions from the other five provinces is 22.4% and 29.5%, respectively, much less than those of local emissions. However, the contribution increases from 37.6% to 54.3% with deterioration of Beijing's air quality from being slightly to severely polluted. The result is consistent with that from Lang et al. (2013), reporting that regional transport accounts for 54.6% of the $PM_{2.5}$ mass in Beijing during a PM pollution episode. Additionally, Jiang et al. (2015) have concluded that the transport from the environs of Beijing contributes about 55% of the peak $PM_{2.5}$ concentration in the city during a severe PM pollution episode occurred in December 2013. Wu et al. (2017) have also shown that 61.5% of the $PM_{2.5}$ mass in Beijing is contributed by regional transport during a summertime PM pollution episode. The contribution of Hebei emissions to the $PM_{2.5}$ mass in Beijing is the most significant, exceeding 20% when Beijing's air quality is not excellent. The contribution of emissions from Tianjin, Henan, Shandong, and Shanxi is generally less than 10% under different pollution levels. However, when Beijing's air quality is severely polluted, the contribution of Shandong emissions is also significant, attaining 16.4%. The background source contributes more than 20% of the $PM_{2.5}$ mass in Beijing when the air quality is excellent and severely polluted, and between 12.8% and 15.4% under the other pollution levels.

The air quality in Tianjin is dominated by trans-boundary transport of air pollutants, with the non-local $PM_{2.5}$ contribution generally higher than 55%, especially when the air

https://doi.org/10.5194/acp-2020-597
Preprint. Discussion started: 14 July 2020

quality is severely polluted, with the non-local $PM_{2.5}$ contribution of 95.9%, which is higher than the average non-local contribution of 44% reported by Meng et al. (2020). The $PM_{2.5}$ contribution of local emissions decreases with the deterioration of the air quality in Tianjin, with average contributions of 44.9%, 41.3%, 37.0%, and 29.6%, respectively, when the air quality is good, slightly, moderately, and heavily polluted. The Hebei emissions play a significant role in the PM pollution in Tianjin, generally contributing more than 25% of $PM_{2.5}$ concentrations, except when the air quality is excellent. Meng et al. (2020) have emphasized the important contribution of Hebei emissions to $PM_{2.5}$ concentrations in Tianjin. However, Meng et al. (2020) have suggested that the $PM_{2.5}$ contribution of local emissions gradually increases with continuous deterioration of the PM pollution, which is different from that in the study. The $PM_{2.5}$ contribution of the background source is between 11.4% to 16.5%, except when the air quality is severely polluted, with the contribution exceeding 30%.

The Hebei's air quality is obviously determined by local emissions when the air quality is excellent or good, with the average $PM_{2.5}$ contribution of 65.8% and 60.9%, respectively. Additionally, the contribution of non-local emissions to the $PM_{2.5}$ mass in Hebei is almost the same as that of local emissions, varying from 46.2% to 54.8% with $PM_{2.5}$ concentrations exceeding 75 μg m^{-3}. The $PM_{2.5}$ contribution of emissions from Tianjin, Henan, and Shanxi is generally less than 10% under different pollution levels. However, the Shandong emissions contribute more than 10% of the $PM_{2.5}$ mass in Hebei when the air quality becomes polluted. Obviously, with occurrence of severe PM pollution in BTH, the contribution of Shandong emissions to the $PM_{2.5}$ mass in BTH becomes considerable, which has also been suggested by Chang et al. (2019). The $PM_{2.5}$ contribution of background source to Hebei decreases with deterioration of the air quality, ranging from 8.2% to 19.2% during the episode. Overall, in Hebei, local emissions generally dominate the $PM_{2.5}$ level under different pollution level, but non-local emissions play a more and more important role with deterioration of PM pollution,

https://doi.org/10.5194/acp-2020-597
Preprint. Discussion started: 14 July 2020

which is consistent with those in Wang et al. (2015) and Wang et al. (2019).

The local and non-local emissions generally play an almost equivalent role in the air quality in Henan when the severe PM pollution does not occur. However, when the air quality is severely polluted, the non-local emissions contribute about 62% of the $PM_{2.5}$ mass. The Shandong emissions generally contribute more $PM_{2.5}$ mass than the other five provinces when the air quality is polluted, with the $PM_{2.5}$ contribution exceeding 10%. The background source accounts for more than 10% with the air quality being excellent or good. In Shandong, the local emissions dominate the air quality, generally contributing more than 60% of the $PM_{2.5}$ mass. The total $PM_{2.5}$ contribution of emissions from Beijing, Tianjin, Hebei, Henan, and Shanxi is less than 30%, and $PM_{2.5}$ contributions of background source range from 10% to 15% under different pollution levels. The air quality in Shanxi is mainly decided by local emissions, with the $PM_{2.5}$ contribution of 58.7%, 57.8%, 43.8%, and 47.7% when the air quality being from excellent, good, slightly, and moderately polluted, respectively. Hebei and Henan emissions contribute more than 10% and 15% of the $PM_{2.5}$ mass in Shanxi, when the air quality is slightly and moderately polluted. The $PM_{2.5}$ contribution of background source is notable, generally exceeding 20%.

Table 4, Table 5 and Figure 10 further show the average contribution of local and non-local emissions to the aerosol species in Beijing, Tianjin, Hebei, Henan, Shandong, and Shanxi during the episode. Interestingly, the local emissions dominate the EC and POA in Beijing, with a contribution of 61.1% and 64.1%. Hu et al. (2015) have also revealed that local emissions constitute the major source of POA in Beijing, particularly during wintertime. Additionally, local emissions also account for around 32% of the SOA in Beijing, and the high organic aerosol contribution is likely caused by emissions of large amounts of vehicles in Beijing. Except for EC and POA, non-local emissions dominate the aerosol species concentration in Beijing, with contributions exceeding 60%, especially for sulfate and nitrate

https://doi.org/10.5194/acp-2020-597
Preprint. Discussion started: 14 July 2020

in which the contribution of non-local emissions is more than 90% (Figure 10). Ying et al. (2014) have shown that the inter-regional transport of air pollutants plays an important role in the secondary aerosols formation during the polluted episode in China. Sun et al. (2016) have also demonstrated that the secondary aerosol formed on a regional scale dominates the aerosol compositions during the haze episode, with an average of 67%. Apparently, the impact of Hebei emissions on PM pollution in Beijing is the most significant, with the nitrate and ammonium contribution exceeding 40% (Table 4). Except for EC and POA, contributions of background source to the aerosol species in Beijing is generally more than 10%. It is worth noting that the nitrate contribution of the background source is 32.1%, which is caused by the slow oxidation of NO_2 during wintertime.

In Tianjin, the non-local emissions play a dominant role in concentrations SOA, sulfate, nitrate, and ammonium, with contributions of 73.6%, 68.6%, 88.7%, and 71.3%, and also account for 48.1% and 50.7% of the EC and POA mass, respectively. In general, Hebei emissions constitute the most important contributor of aerosol species in the non-local sources, followed by Shandong emissions. In Hebei, the local emissions determine the levels of EC, POA, sulfate, and ammonium, with contributions of 73.8%, 63.0%, 64.3%, and 67.4%, respectively. The SOA mass is mainly contributed by local (49.4%) and Shandong (16.7%) emissions, and background sources (11.6%). However, the non-local emissions dominate the nitrate mass in Hebei, with the contribution of 78.7%, most of which is from Henan (11.4%), Shandong (14.6%), Shanxi (10.8%), and background sources (22.9%). Except for sulfate, the aerosol species in Henan are generally controlled by local emissions, with contributions varying from 45% to 65%. The sulfate contribution of non-local emissions is 83.2%, mainly contributed by Hebei (16.7%), Shandong (14.9%), Shanxi (12.1%), and background (22%). The local emissions contribute about 60~80% of the aerosol species mass in Shandong, except nitrate aerosols, which are dominated by non-local emissions with a contribution of

https://doi.org/10.5194/acp-2020-597
Preprint. Discussion started: 14 July 2020

75.1%. More than 60% of EC, POA, sulfate and ammonium in Shanxi are formed from local emissions, but the non-local emissions are the dominant contributor to SOA and nitrate concentrations.

4 Summary and conclusions

We have developed a source-oriented WRF-Chem model, treating the precursors of aerosols from different sources and their corresponding reaction products as different species and tracked independently in chemical, physical, and dynamic processes. The model is used to evaluate contributions of local and non-local emissions to the PM pollution in the NCP, including Beijing, Tianjin, Hebei, Henan, and Shandong, as well as the adjacent province on the west, Shanxi during a persistent and severe haze episode from 05 December 2015 to 04 January 2016. The model exhibits good performance in predicting the temporal variation and spatial distribution of air pollutants in the NCP and also reasonably simulates the aerosol species against measurements in Beijing.

As two megacities in the NCP, Beijing and Tianjin have made great efforts to decrease local emissions of air pollutants since 2013, such as replace residential coal use with gas and electricity, elevating vehicle emissions standards, phasing out high-emitting industries, etc. (Zhang et al., 2019). However, heavy PM pollutions still occur in the two cities, which is mainly resulted from trans-boundary transport of air pollutants. Simulations of the source-oriented WRF-Chem model reveal that, on average local and non-local emissions contribute 36.3% and 63.7% of the $PM_{2.5}$ mass in Beijing during the episode. When the air quality is excellent or good in terms of hourly $PM_{2.5}$ concentrations, the local emissions contribute more than 50% to the $PM_{2.5}$ mass, dominating Beijing's air quality. However, with deterioration of Beijing's air quality from being slightly to severely polluted, the $PM_{2.5}$ contribution of local emissions decreases from 48.7% to 25.1%, indicating the significant

https://doi.org/10.5194/acp-2020-597
Preprint. Discussion started: 14 July 2020

contribution of trans-boundary transport to the PM pollution in Beijing. The non-local emissions account for 76.2% of the $PM_{2.5}$ mass in Tianjin and the contribution exceeds 90% when the air quality is severely polluted. The $PM_{2.5}$ concentrations in three industrialized provinces, Hebei, Shandong, and Henan in the NCP, are generally dominated by the local emissions under different pollution levels, particularly in Shandong with the $PM_{2.5}$ contribution of local emissions exceeding 60%. Efficient emission mitigations of air pollutants in the three provinces need to be carried out continuously to lower PM levels. However, when severe PM pollution occurs, the $PM_{2.5}$ contribution of local emissions in Hebei and Henan decreases considerably. The impact of Shanxi's emissions on $PM_{2.5}$ concentrations in the NCP is generally not significant.

The primary aerosol species, such as EC and POA, are generally controlled by local emissions with the average contribution ranging from about 50% to 85% in the six provinces. However, the source apportionment of secondary aerosols shows large differences during the episode, with more evident regional characteristics. Local emissions contribute more than 60% of the SOA mass in Shandong, 40~50% in Hebei, Henan and Shanxi, and around 30% in Beijing and Tianjin. The sulfate contribution of local emissions is significant in Hebei, Shandong and Shanxi, exceeding 60%, but less than 10% in Beijing. Except in Henan, local emissions do not play an important role in the nitrate formation, with contributions less than 30%, and most of nitrate aerosols are produced during trans-boundary transport of its precursors. Ammonium aerosols in Beijing and Tianjin are mainly determined by non-local emissions, with the contribution of around 70%. Local emissions in the other four provinces account for around 60% of the ammonium mass.

In order to reduce PM pollution, the cooperation to carry out strict emission mitigation measures is critical for all provinces, especially with regard to Beijing and Tianjin. In Beijing and Tianjin, reducing direct emissions of primary aerosols, such as EC and POA, constitutes

https://doi.org/10.5194/acp-2020-597
Preprint. Discussion started: 14 July 2020

the priority, and more efforts need to be made to reduce local emissions of air pollutants in Hebei, Henan, Shandong, and Shanxi.

Competing interests. The authors declare no competing financial interest.

Data availability. The real-time $PM_{2.5}$, O_3, NO_2, SO_2 and CO observations are accessible for the public on the following website: http://106.37.208. 233:20035/ (last access: 24 November 2019) (China MEP, 2013a). One can also access the historic profile of observed ambient pollutants by visiting http://www.aqistudy.cn/ (last access: 24 November 2019) (China MEP, 2013b).

Author contribution. Guohui Li, as the contact author, provided the ideas and financial support, developed the model code, verified the conclusions, and revised the paper. Jiarui Wu conducted a research, designed the experiments, performed the simulation, processed the data, prepared the data visualization, and prepared the manuscript with contributions from all authors. Naifang Bei validated the model performance, analyzed the study data, and reviewed the manuscript. Yuan Wang validated the model performance, verified the results and provided the critical reviews. Suixin Liu provided the data and the primary data process, and reviewed the manuscript. Xia Li, Lang Liu, Ruonan Wang, Jiaoyang Yu and Min Zuo analyzed the initial simulation data, visualized the model results and reviewed the paper. Zhenxing Shen, Junji Cao and Xuexi Tie provided critical reviews pre-publication stage.

Acknowledgements. This work is financially supported by the National Key R&D Plan (Quantitative Relationship and Regulation Principle between Regional Oxidation Capacity of Atmospheric and Air Quality (2017YFC0210000)) and National Research Program for Key Issues in Air Pollution Control (DQGG0105).

https://doi.org/10.5194/acp-2020-597
Preprint. Discussion started: 14 July 2020

References

An, Z. S., Huang, R. J., Zhang, R. Y., Tie, X. X., Li, G. H., Cao, J. J., Zhou, W. J., Shi, Z. G., Han, Y. M., Gu, Z. L., and Ji, Y. M.: Severe haze in northern China: A synergy of anthropogenic emissions and atmospheric processes, P. Natl. Acad. Sci. USA., 116, 8657-8666, doi: 10.1073/pnas.1900125116, 2019.

Bei, N. F., Wu, J. R., Elser, M., Feng, T., Cao, J. J., El-Haddad, I., Li, X., Huang, R. J., Li, Z. Q., Long, X., Xing, L., Zhao, S. Y., Tie, X. X., Prevot, A. S. H., and Li, G. H.: Impacts of meteorological uncertainties on the haze formation in Beijing-Tianjin-Hebei (BTH) during wintertime: a case study, Atmos. Chem. Phys., 17, 14579-14591, 10.5194/acp-17-14579-2017, 2017.

Binkowski, F. S., and Roselle, S. J.: Models-3 community multiscale air quality (CMAQ) model aerosol component - 1. Model description, J. Geophys. Res. Atmos., 108, 18, doi: 10.1029/2001jd001409, 2003.

Burr, M. J., and Zhang, Y.: Source apportionment of fine particulate matter over the Eastern U.S. Part II: source apportionment simulations using CAMx/PSAT and comparisons with CMAQ source sensitivity simulations, Atmos. Pollut. Res., 2, 318-336, doi: 10.5094/apr.2011.037, 2011.

Carter, W. P. L.: Development of the SAPRC-07 chemical mechanism, Atmos. Environ., 44, 5324-5335, doi: 10.1016/j.atmosenv.2010.01.026, 2010.

Chang, X., Wang, S. X., Zhao, B., Xing, J., Liu, X. X., Wei, L., Song, Y., Wu, W. J., Cai, S. Y., Zheng, H. T., Ding, D., and Zheng, M.: Contributions of inter-city and regional transport to $PM_{2.5}$ concentrations in the Beijing-Tianjin-Hebei region and its implications on regional joint air pollution control, Sci. Total Environ., 660, 1191-1200, 10.1016/j.scitotenv.2018.12.474, 2019.

Chen, F., and Dudhia, J.: Coupling an advanced land surface-hydrology model with the Penn State-NCAR MM5 modeling system. Part I: Model implementation and sensitivity, Mon. Weather. Rev., 129, 569-585, doi: 10.1175/1520-0493(2001)129<0569:caalsh>2.0.co;2, 2001.

China MEP (Ministry of Environmental Protection, China): Air Quality Observation Real-time Release Platform of MEP Data Center, available at: http://106.37.208.233:20035/ (last access: 24 November 2019), 2013a.

China MEP (Ministry of Environmental Protection, China): On- line Monitoring and Analysis Platform of China Air Quality, available at: http://www.aqistudy.cn/ (last access: 24 November 2019), 2013b.

Chou, M.-D. and Suarez, M. J.: A solar radiation parameterization for atmospheric studies, NASA Tech. Rep. NASA/TM-1999- 10460, Vol. 15, 38 pp., 1999.

Chou, M.-D. and Suarez, M. J.: A thermal infrared radiation parameterization for atmospheric studies, NASA/TM-2001-104606, Vol. 19, 55 pp., 2001.

Cooper, J. A., and Watson, J. G.: Receptor oriented methods of air particulate source apportionment, J. Air. Pollut. Control. Assoc., 30, 1116-1125, doi: 10.1080/00022470.1980.10465157, 1980.

Donahue, N. M., Robinson, A. L., Stanier, C. O., and Pandis, S. N.: Coupled partitioning, dilution, and chemical aging of semivolatile organics, Environ. Sci. Technol., 40,

2635-2643, doi: 10.1021/es052297c, 2006.

Dong, Z., Wang, S., Xing, J., Chang, X., Ding, D., and Zheng, H.: Regional transport in Beijing-Tianjin-Hebei region and its changes during 2014–2017: The impacts of meteorology and emission reduction, Sci. Total Environ., 737, 139792, https://doi.org/10.1016/j.scitotenv.2020.139792, 2020.

Feng, T., Bei, N. F., Huang, R. J., Cao, J. J., Zhang, Q., Zhou, W. J., Tie, X. X., Liu, S. X., Zhang, T., Su, X. L., Lei, W. F., Molina, L. T., and Li, G. H.: Summertime ozone formation in Xi'an and surrounding areas, China, Atmos. Chem. Phys., 16, 4323-4342, doi: 10.5194/acp-16-4323-2016, 2016.

Foley, K. M., Roselle, S. J., Appel, K. W., Bhave, P. V., Pleim, J. E., Otte, T. L., Mathur, R., Sarwar, G., Young, J. O., Gilliam, R. C., Nolte, C. G., Kelly, J. T., Gilliland, A. B., and Bash, J. O.: Incremental testing of the Community Multiscale Air Quality (CMAQ) modeling system version 4.7, Geosci. Model. Dev., 3, 205-226, doi: 10.5194/gmd-3-205-2010, 2010.

Grell, G. A., and Devenyi, D.: A generalized approach to parameterizing convection combining ensemble and data assimilation techniques, Geophys. Res. Lett., 29, 4, doi: 10.1029/2002gl015311, 2002.

Grell, G. A., Peckham, S. E., Schmitz, R., McKeen, S. A., Frost, G., Skamarock, W. C., and Eder, B.: Fully coupled "online" chemistry within the WRF model, Atmos. Environ., 39, 6957-6975, doi: 10.1016/j.atmosenv.2005.04.027, 2005.

Guenther, A., Karl, T., Harley, P., Wiedinmyer, C., Palmer, P. I., and Geron, C.: Estimates of global terrestrial isoprene emissions using MEGAN (Model of Emissions of Gases and Aerosols from Nature), Atmos. Chem. Phys., 6, 3181-3210, doi: 10.5194/acp-6-3181-2006, 2006a.

Guenther, A., Karl, T., Harley, P., Wiedinmyer, C., Palmer, P. I., and Geron, C.: Estimates of global terrestrial isoprene emissions using MEGAN (Model of Emissions of Gases and Aerosols from Nature), Atmos. Chem. Phys., 6, 3181-3210, 2006b.

Guo, S., Hu, M., Wang, Z. B., Slanina, J., and Zhao, Y. L.: Size-resolved aerosol water-soluble ionic compositions in the summer of Beijing: implication of regional secondary formation, Atmos. Chem. Phys., 10, 947-959, doi: 10.5194/acp-10-947-2010, 2010.

Guo, S., Hu, M., Zamora, M. L., Peng, J. F., Shang, D. J., Zheng, J., Du, Z. F., Wu, Z., Shao, M., Zeng, L. M., Molina, M. J., and Zhang, R. Y.: Elucidating severe urban haze formation in China, P. Natl. Acad. Sci. USA., 111, 17373-17378, doi: 10.1073/pnas.1419604111, 2014.

Hess, P. G., Flocke, S., Lamarque, J. F., Barth, M. C., and Madronich, S.: Episodic modeling of the chemical structure of the troposphere as revealed during the spring MLOPEX 2 intensive, J. Geophys. Res. Atmos., 105, 26809-26839, doi: 10.1029/2000jd900253, 2000.

Hong, S.-Y., and Lim, J.-O. J.: The WRF Single-Moment 6-Class Microphysics Scheme (WSM6), Asia-Pac. J. Atmos. Sci., 42, 129-151, 2006.

Horowitz, L. W., Walters, S., Mauzerall, D. L., Emmons, L. K., Rasch, P. J., Granier, C., Tie, X. X., Lamarque, J. F., Schultz, M. G., Tyndall, G. S., Orlando, J. J., and Brasseur, G. P.:

https://doi.org/10.5194/acp-2020-597
Preprint. Discussion started: 14 July 2020

A global simulation of tropospheric ozone and related tracers: Description and evaluation of MOZART, version 2, J. Geophys. Res. Atmos., 108, 29, doi: 10.1029/2002jd002853, 2003.

Hu, J. L., Wu, L., Zheng, B., Zhang, Q., He, K. B., Chang, Q., Li, X. H., Yang, F. M., Ying, Q., and Zhang, H. L.: Source contributions and regional transport of primary particulate matter in China, Environ. Pollut., 207, 31-42, doi: 10.1016/j.envpol.2015.08.037, 2015.

Janjić, Z. I.: Nonsingular Implementation of the Mellor–Yamada Level 2.5 Scheme in the NCEP Meso Model, Ncep Office Note, 436, 2002.

Jiang, C., Wang, H., Zhao, T., Li, T., and Che, H.: Modeling study of $PM_{2.5}$ pollutant transport across cities in China's Jing-Jin- Ji region during a severe haze episode in December 2013, Atmos. Chem. Phys., 15, 5803–5814, doi:10.5194/acp-15-5803-2015, 2015.

Lang, J. L., Cheng, S. Y., Li, J. B., Chen, D. S., Zhou, Y., Wei, X., Han, L. H., and Wang, H. Y.: A Monitoring and Modeling Study to Investigate Regional Transport and Characteristics of $PM_{2.5}$ Pollution, Aerosol. Air. Qual. Res., 13, 943-956, doi: 10.4209/aaqr.2012.09.0242, 2013.

Li, G., Lei, W., Zavala, M., Volkamer, R., Dusanter, S., Stevens, P., and Molina, L. T.: Impacts of HONO sources on the photochemistry in Mexico City during the MCMA-2006/MILAGO Campaign, Atmos. Chem. Phys., 10, 6551-6567, doi: 10.5194/acp-10-6551-2010, 2010.

Li, G., Bei, N., Tie, X., and Molina, L. T.: Aerosol effects on the photochemistry in Mexico City during MCMA-2006/MILAGRO campaign, Atmos. Chem. Phys., 11, 5169-5182, doi: 10.5194/acp-11-5169-2011, 2011a.

Li, G., Zavala, M., Lei, W., Tsimpidi, A. P., Karydis, V. A., Pandis, S. N., Canagaratna, M. R., and Molina, L. T.: Simulations of organic aerosol concentrations in Mexico City using the WRF-CHEM model during the MCMA-2006/MILAGRO campaign, Atmos. Chem. Phys., 11, 3789-3809, doi: 10.5194/acp-11-3789-2011, 2011b.

Li, G. H., Zhang, R. Y., Fan, J. W., and Tie, X. X.: Impacts of black carbon aerosol on photolysis and ozone, J. Geophys. Res. Atmos., 110, 10, doi: 10.1029/2005jd005898, 2005.

Li, G. H., Bei, N. F., Cao, J. J., Wu, J. R., Long, X., Feng, T., Dai, W. T., Liu, S. X., Zhang, Q., and Tie, X. X.: Widespread and persistent ozone pollution in eastern China during the non-winter season of 2015: observations and source attributions, Atmos. Chem. Phys., 17, 2759-2774, doi: 10.5194/acp-17-2759-2017, 2017.

Li, P. F., Yan, R. C., Yu, S. C., Wang, S., Liu, W. P., and Bao, H. M.: Reinstate regional transport of PM2.5 as a major cause of severe haze in Beijing, P. Natl. Acad. Sci. USA., 112, E2739-E2740, doi: 10.1073/pnas.1502596112, 2015.

Li, X., Wu, J. R., Elser, M., Feng, T., Cao, J. J., El-Haddad, I., Huang, R. J., Tie, X. X., Prevot, A. S. H., and Li, G. H.: Contributions of residential coal combustion to the air quality in Beijing-Tianjin-Hebei (BTH), China: a case study, Atmos. Chem. Phys., 18, 10675-10691, 10.5194/acp-18-10675-2018, 2018.

Lipsky, E. M., and Robinson, A. L.: Effects of dilution on fine particle mass and partitioning of semivolatile organics in diesel exhaust and wood smoke, Environ. Sci. Technol., 40,

155-162, doi: 10.1021/es050319p, 2006.

Liu, L., Wang, L., Bai, Y., Yang, H., Lin, C., Kong, H., Ma, S., and Wang, J.: Simulation for the impacts of regional transport on winter particulate matter levels over Henan based on WRF/Chem model, Acta Scientiae Circumstantiae, 37, 1843-1854, 2017.

Long, X., Tie, X. X., Cao, J. J., Huang, R. J., Feng, T., Li, N., Zhao, S. Y., Tian, J., Li, G. H., and Zhang, Q.: Impact of crop field burning and mountains on heavy haze in the North China Plain: a case study, Atmos. Chem. Phys., 16, 9675-9691, doi: 10.5194/acp-16-9675-2016, 2016.

Marmur, A., Unal, A., Mulholland, J. A., and Russell, A. G.: Optimization-based source apportionment of $PM_{2.5}$ incorporating gas-to-particle ratios, Environ. Sci. Technol., 39, 3245-3254, doi: 10.1021/es0490121, 2005.

Marmur, A., Park, S. K., Mulholland, J. A., Tolbert, P. E., and Russell, A. G.: Source apportionment of $PM_{2.5}$ in the southeastern United States using receptor and emissions-based models: Conceptual differences and implications for time-series health studies, Atmos. Environ., 40, 2533-2551, doi: 10.1016/j.atmosenv.2005.12.019, 2006.

Meng, L., Cai, Z., Li, Y., Hao, J., and Wang, X.: Spatial and Temporal Distributions and Source Simulation during Heavy Pollution of $PM_{2.5}$ in Tianjin City, Research of Environmental Sciences, 33, 9-17, 2020.

Nenes, A., Pandis, S. N., and Pilinis, C.: ISORROPIA: A new thermodynamic equilibrium model for multiphase multicomponent inorganic aerosols, Aquat. Geochem., 4, 123-152, doi: 10.1023/a:1009604003981, 1998.

Odum, J. R., Hoffmann, T., Bowman, F., Collins, D., Flagan, R. C., and Seinfeld, J. H.: Gas/particle partitioning and secondary organic aerosol yields, Environ. Sci. Technol., 30, 2580-2585, doi: 10.1021/es950943+, 1996.

Paatero, P., and Tapper, U.: Analysis of different modes of factor-analysis as least-squares fit problems, Chemometrics Intell. Lab. Syst., 18, 183-194, doi: 10.1016/0169-7439(93)80055-m, 1993.

Pankow, J. F.: An absorption-model of the gas aerosol partitioning involved in the formation of secondary organic aerosol, Atmos. Environ., 28, 189-193, doi: 10.1016/1352-2310(94)90094-9, 1994.

Robinson, A. L., Donahue, N. M., Shrivastava, M. K., Weitkamp, E. A., Sage, A. M., Grieshop, A. P., Lane, T. E., Pierce, J. R., and Pandis, S. N.: Rethinking organic aerosols: Semivolatile emissions and photochemical aging, Science., 315, 1259-1262, doi: 10.1126/science.1133061, 2007.

Shrivastava, M. K., Lipsky, E. M., Stanier, C. O., and Robinson, A. L.: Modeling semivolatile organic aerosol mass emissions from combustion systems, Environ. Sci. Technol., 40, 2671-2677, doi: 10.1021/es0522231, 2006.

Shrivastava, M. K., Lane, T. E., Donahue, N. M., Pandis, S. N., and Robinson, A. L.: Effects of gas particle partitioning and aging of primary emissions on urban and regional organic aerosol concentrations, J. Geophys. Res. Atmos., 113, 16, doi: 10.1029/2007jd009735, 2008.

Sun, Y. L., Chen, C., Zhang, Y. J., Xu, W. Q., Zhou, L. B., Cheng, X. L., Zheng, H. T., Ji, D. S., Li, J., Tang, X., Fu, P. Q., and Wang, Z. F.: Rapid formation and evolution of an

https://doi.org/10.5194/acp-2020-597
Preprint. Discussion started: 14 July 2020

extreme haze episode in Northern China during winter 2015, Sci. Rep., 6, 9, doi: 10.1038/srep27151, 2016.

Tsimpidi, A. P., Karydis, V. A., Zavala, M., Lei, W., Molina, L., Ulbrich, I. M., Jimenez, J. L., and Pandis, S. N.: Evaluation of the volatility basis-set approach for the simulation of organic aerosol formation in the Mexico City metropolitan area, Atmos. Chem. Phys., 10, 525-546, doi: 10.5194/acp-10-525-2010, 2010.

Volkamer, R., Martini, F. S., Molina, L. T., Salcedo, D., Jimenez, J. L., and Molina, M. J.: A missing sink for gas-phase glyoxal in Mexico City: Formation of secondary organic aerosol, Geophys. Res. Lett., 34, 5, doi: 10.1029/2007gl030752, 2007.

Wagstrom, K. M., Pandis, S. N., Yarwood, G., Wilson, G. M., and Morris, R. E.: Development and application of a computationally efficient particulate matter apportionment algorithm in a three-dimensional chemical transport model, Atmos. Environ., 42, 5650-5659, doi: 10.1016/j.atmosenv.2008.03.012, 2008.

Wang, L. T., Wei, Z., Wei, W., Fu, J. S., Meng, C. C., and Ma, S. M.: Source apportionment of $PM_{2.5}$ in top polluted cities in Hebei, China using the CMAQ model, Atmos. Environ., 122, 723-736, 10.1016/j.atmosenv.2015.10.041, 2015.

Wang, Q., Luo, K., Fan, J. R., Gao, X., and Cen, K. F.: Spatial Distribution and Multiscale Transport Characteristics of $PM_{2.5}$ in China, Aerosol Air Qual. Res., 19, 1993-2007, 10.4209/aaqr.2019.04.0202, 2019.

Wang, Z. S., Chien, C. J., and Tonnesen, G. S.: Development of a tagged species source apportionment algorithm to characterize three-dimensional transport and transformation of precursors and secondary pollutants, J. Geophys. Res. Atmos., 114, 17, doi: 10.1029/2008jd010846, 2009.

Wesely, M. L.: Parameterization of surface resistances to gaseous dry deposition in regional-scale numerical models , Atmos. Environ., 23, 1293-1304, 1989.

Wu, J. R., Li, G. H., Cao, J. J., Bei, N. F., Wang, Y. C., Feng, T., Huang, R. J., Liu, S. X., Zhang, Q., and Tie, X. X.: Contributions of trans-boundary transport to summertime air quality in Beijing, China, Atmos. Chem. Phys., 17, 2035-2051, doi: 10.5194/acp-17-2035-2017, 2017.

Wu, J. R., Bei, N. F., Hu, B., Liu, S. X., Wang, Y., Shen, Z. X., Li, X., Liu, L., Wang, R. N., Liu, Z. R., Cao, J. J., Tie, X. X., Molina, L. T., and Li, G. H.: Aerosol-photolysis interaction reduces particulate matter during wintertime haze events, P. Natl. Acad. Sci. USA., 117, 9755-9761, 10.1073/pnas.1916775117, 2020.

Ying, Q., and Kleeman, M. J.: Source contributions to the regional distribution of secondary particulate matter in California, Atmos. Environ., 40, 736-752, doi: 10.1016/j.atmosenv.2005.10.007, 2006.

Ying, Q., Lu, J., Allen, P., Livingstone, P., Kaduwela, A., and Kleeman, M.: Modeling air quality during the California Regional $PM_{10}/PM_{2.5}$ Air Quality Study (CRPAQS) using the UCD/CIT source-oriented air quality model - Part I. Base case model results, Atmos. Environ., 42, 8954-8966, doi: 10.1016/j.atmosenv.2008.05.064, 2008a.

Ying, Q., Lu, J., Kaduwela, A., and Kleeman, M.: Modeling air quality during the California Regional $PM_{10}/PM_{2.5}$ Air Quality Study (CPRAQS) using the UCD/CIT Source Oriented Air Quality Model - Part II. Regional source apportionment of primary airborne

particulate matter, Atmos. Environ., 42, 8967-8978, doi: 10.1016/j.atmosenv.2008.05.065, 2008b.

Ying, Q., Wu, L., and Zhang, H. L.: Local and inter-regional contributions to $PM_{2.5}$ nitrate and sulfate in China, Atmos. Environ., 94, 582-592, doi: 10.1016/j.atmosenv.2014.05.078, 2014.

Zamora, M. L., Peng, J., Hu, M., Guo, S., Marrero-Ortiz, W., Shang, D., Zheng, J., Du, Z., Wu, Z., and Zhang, R.: Wintertime aerosol properties in Beijing, Atmos. Chem. Phys., 19, 14329-14338, doi: 10.5194/acp-19-14329-2019, 2019.

Zhang, H., DeNero, S. P., Joe, D. K., Lee, H. H., Chen, S. H., Michalakes, J., and Kleeman, M. J.: Development of a source oriented version of the WRF/Chem model and its application to the California regional $PM_{10}/PM_{2.5}$ air quality study, Atmos. Chem. Phys., 14, 485-503, doi: 10.5194/acp-14-485-2014, 2014.

Zhang, H. L., and Ying, Q.: Source apportionment of airborne particulate matter in Southeast Texas using a source-oriented 3D air quality model, Atmos. Environ., 44, 3547-3557, doi: 10.1016/j.atmosenv.2010.06.004, 2010.

Zhang, H. L., and Ying, Q.: Secondary organic aerosol formation and source apportionment in Southeast Texas, Atmos. Environ., 45, 3217-3227, doi: 10.1016/j.atmosenv.2011.03.046, 2011.

Zhang, Q., Streets, D. G., Carmichael, G. R., He, K. B., Huo, H., Kannari, A., Klimont, Z., Park, I. S., Reddy, S., Fu, J. S., Chen, D., Duan, L., Lei, Y., Wang, L. T., and Yao, Z. L.: Asian emissions in 2006 for the NASA INTEX-B mission, Atmos. Chem. Phys., 9, 5131-5153, 2009.

Zhang, Q., Zheng, Y. X., Tong, D., Shao, M., Wang, S. X., Zhang, Y. H., Xu, X. D., Wang, J. N., He, H., Liu, W. Q., Ding, Y. H., Lei, Y., Li, J. H., Wang, Z. F., Zhang, X. Y., Wang, Y. S., Cheng, J., Liu, Y., Shi, Q. R., Yan, L., Geng, G. N., Hong, C. P., Li, M., Liu, F., Zheng, B., Cao, J. J., Ding, A. J., Gao, J., Fu, Q. Y., Huo, J. T., Liu, B. X., Liu, Z. R., Yang, F. M., He, K. B., and Hao, J. M.: Drivers of improved $PM_{2.5}$ air quality in China from 2013 to 2017, P. Natl. Acad. Sci. USA., 116, 24463-24469, 10.1073/pnas.1907956116, 2019.

Zhang, R. Y., Guo, S., Zamora, M. L., and Hu, M.: Reply to Li et al.: Insufficient evidence for the contribution of regional transport to severe haze formation in Beijing, P. Natl. Acad. Sci. USA., 112, E2741-E2741, doi: 10.1073/pnas.1503855112, 2015.

Zheng, B., Tong, D., Li, M., Liu, F., Hong, C. P., Geng, G. N., Li, H. Y., Li, X., Peng, L. Q., Qi, J., Yan, L., Zhang, Y. X., Zhao, H. Y., Zheng, Y. X., He, K. B., and Zhang, Q.: Trends in China's anthropogenic emissions since 2010 as the consequence of clean air actions, Atmos. Chem. Phys., 18, 14095-14111, 10.5194/acp-18-14095-2018, 2018.

Zhao, J., Levitt, N. P., Zhang, R. Y., and Chen, J. M.: Heterogeneous reactions of methylglyoxal in acidic media: Implications for secondary organic aerosol formation, Environ. Sci. Technol., 40, 7682-7687, doi: 10.1021/es060610k, 2006.

https://doi.org/10.5194/acp-2020-597
Preprint. Discussion started: 14 July 2020

Table 1 WRF-Chem model configurations.

Region	North China Plain
Simulation period	05 December 2015 to 04 January 2016
Domain size	300 × 300
Domain center	38°N, 116°E
Horizontal resolution	6 km × 6 km
Vertical resolution	35 vertical levels with a stretched vertical grid with spacing ranging from 30 m near the surface, to 500 m at 2.5 km and 1 km above 14 km
Microphysics scheme	WSM 6-class graupel scheme (Hong and Lim, 2006)
Cumulus scheme	Grell-Devenyi ensemble scheme (Grell and Devenyi, 2002)
Boundary layer scheme	MYJ TKE scheme(Janjić, 2002)
Surface layer scheme	MYJ surface scheme (Janjić, 2002)
Land-surface scheme	Unified Noah land-surface model (Chen and Dudhia, 2001)
Longwave radiation scheme	Goddard longwave scheme (Chou and Suarez, 2001)
Shortwave radiation scheme	Goddard shortwave scheme (Chou and Suarez, 1999)
Meteorological boundary and initial conditions	NCEP 1°×1° reanalysis data
Chemical initial and boundary conditions	MOZART 6-hour output (Horowitz et al., 2003)
Anthropogenic emission inventory	Developed by Zhang et al. (2009) and Li et al. (2017), 2012 base year, and SAPRC-99 chemical mechanism
Biogenic emission inventory	Online MEGAN model developed by Guenther et al. (2006)

https://doi.org/10.5194/acp-2020-597
Preprint. Discussion started: 14 July 2020

Table 2 Average $PM_{2.5}$ contributions (%) in Beijing, Tianjin, and Hebei under different pollution levels from local, the other five provinces, and background source from 05 December 2015 to 04 January 2016.

Pollution Level (μg m^{-3})	0-35	35-75	75-115	115-150	150-250	>250
Beijing						
Beijing	56.8	55.0	48.7	40.5	35.4	25.1
Tianjin	1.1	3.7	5.2	9.3	8.0	8.0
Hebei	16.9	20.4	24.8	28.4	28.4	21.2
Henan	1.1	1.2	1.8	1.4	3.4	6.2
Shandong	1.1	1.2	2.0	2.4	7.1	16.4
Shanxi	2.2	3.0	3.8	2.9	4.8	2.5
Background	20.8	15.4	13.8	15.1	12.8	20.6
Tianjin						
Beijing	21.6	7.8	5.7	5.9	7.8	8.8
Tianjin	36.5	44.9	41.3	37.0	29.6	4.1
Hebei	23.1	28.3	30.4	31.7	30.6	27.8
Henan	0.8	1.1	1.3	2.1	3.7	6.7
Shandong	0.8	2.0	3.6	6.2	13.9	18.0
Shanxi	0.8	1.3	1.6	2.3	3.0	4.1
Background	16.5	14.6	16.0	14.9	11.4	30.5
Hebei						
Beijing	4.1	5.7	5.7	6.2	5.0	5.8
Tianjin	2.7	5.2	5.3	5.5	5.4	6.7
Hebei	65.8	60.9	53.8	50.3	45.2	49.0
Henan	0.9	3.1	5.4	5.8	9.3	6.7
Shandong	0.9	5.4	11.3	12.7	18.0	18.6
Shanxi	6.4	4.4	5.4	5.6	5.7	5.1
Background	19.2	15.2	13.1	13.9	11.3	8.2

https://doi.org/10.5194/acp-2020-597
Preprint. Discussion started: 14 July 2020

Table 3 Same as Table 2, but for Henan, Shandong, and Shanxi.

Pollution Level (μg m^{-3})	0-35	35-75	75-115	115-150	150-250	>250
			Henan			
Beijing	0.1	1.2	1.5	2.2	2.4	2.7
Tianjin	0.2	1.2	1.5	2.3	2.3	3.1
Hebei	2.4	4.1	6.9	9.2	12.1	18.3
Henan	55.2	55.3	55.3	50.1	45.5	38.0
Shandong	2.8	6.5	11.3	13.5	13.1	20.0
Shanxi	12.9	8.2	4.7	5.0	5.0	5.9
Background	26.3	23.5	18.8	17.7	19.7	11.9
			Shandong			
Beijing	4.2	1.8	2.7	2.4	3.0	2.2
Tianjin	3.8	2.0	3.2	2.4	3.3	2.2
Hebei	11.8	11.5	9.6	5.5	9.6	5.2
Henan	3.5	3.5	4.4	6.1	8.6	10.1
Shandong	59.2	64.2	62.3	69.7	61.7	66.5
Shanxi	3.8	2.6	2.8	2.5	3.6	3.4
Background	13.8	14.4	15.2	11.3	10.3	10.3
			Shanxi			
Beijing	1.3	1.6	1.6	1.2	/	/
Tianjin	1.3	1.2	1.4	1.0	/	/
Hebei	1.8	7.2	10.3	10.0	/	/
Henan	1.8	7.9	18.0	17.7	/	/
Shandong	1.3	1.9	3.4	2.7	/	/
Shanxi	58.7	57.8	43.8	47.7	/	/
Background	33.6	22.3	21.5	19.7	/	/

https://doi.org/10.5194/acp-2020-597
Preprint. Discussion started: 14 July 2020

Table 4 Average aerosol constituent contributions (%) in Beijing, Tianjin, and Hebei from local, the other five, and background source from 05 December 2015 to 04 January 2016.

Species	EC	POA	SOA	Sulfate	Nitrate	Ammonium
			Beijing			
Beijing	61.1	64.1	31.9	9.8	10.0	32.5
Tianjin	5.1	7.0	8.5	7.8	8.6	7.5
Hebei	24.9	19.0	29.1	48.0	19.1	40.8
Henan	0.6	0.7	2.1	3.9	8.6	2.5
Shandong	2.3	3.2	7.1	9.8	10.5	5.0
Shanxi	1.3	2.1	3.5	7.8	11.0	1.7
Background	4.6	3.9	17.7	12.7	32.1	10.0
			Tianjin			
Beijing	5.3	7.1	13.8	1.1	10.2	3.4
Tianjin	51.9	49.3	26.4	31.4	11.3	28.7
Hebei	23.7	18.7	23.8	27.7	19.4	31.5
Henan	2.3	2.8	5.2	6.5	11.1	6.8
Shandong	9.8	15.3	20.7	20.3	16.7	17.5
Shanxi	1.3	1.5	2.6	4.4	10.6	0.8
Background	5.9	5.3	7.5	8.6	20.6	11.2
			Hebei			
Beijing	4.4	7.2	6.0	0.8	9.4	2.4
Tianjin	3.7	4.8	5.3	3.1	9.5	3.2
Hebei	73.8	63.0	49.4	64.3	21.3	67.4
Henan	4.1	5.9	7.8	9.2	11.4	9.3
Shandong	6.5	11.4	16.7	12.6	14.6	9.7
Shanxi	2.4	3.0	3.2	5.0	10.8	1.2
Background	5.0	4.8	11.6	4.9	22.9	6.9

https://doi.org/10.5194/acp-2020-597
Preprint. Discussion started: 14 July 2020

Table 5 Same as Table 4, but for Henan, Shandong, and Shanxi.

Species	EC	POA	SOA	Sulfate	Nitrate	Ammonium
			Henan			
Beijing	0.6	0.5	1.1	8.7	0.2	0.6
Tianjin	0.7	0.6	0.8	8.7	0.4	0.7
Hebei	16.5	11.9	13.9	16.7	14.4	16.5
Henan	56.5	59.2	45.0	16.8	64.3	56.5
Shandong	8.6	12.1	14.4	14.9	7.9	8.6
Shanxi	5.4	6.1	4.9	12.1	2.0	5.4
Background	11.7	9.5	19.8	22.0	10.8	11.7
			Shandong			
Beijing	1.0	1.0	2.1	0.2	10.1	0.5
Tianjin	1.1	1.0	1.4	1.0	10.5	0.8
Hebei	7.5	4.5	6.5	7.1	16.5	7.3
Henan	5.1	5.1	7.9	8.7	13.8	10.2
Shandong	71.9	78.2	60.4	68.3	24.9	62.5
Shanxi	1.5	1.3	2.0	3.4	11.7	0.7
Background	11.8	8.9	19.6	11.3	12.6	18.0
			Shanxi			
Beijing	0.4	0.4	1.5	0.1	7.1	0.3
Tianjin	0.2	0.2	4.0	0.2	6.6	0.3
Hebei	5.3	3.2	8.6	5.5	13.7	9.3
Henan	4.9	4.4	14.1	10.4	15.3	16.3
Shandong	0.7	0.8	2.5	1.3	8.5	1.8
Shanxi	79.8	84.1	42.1	74.7	19.4	62.2
Background	8.8	6.8	27.1	7.8	29.5	9.7

https://doi.org/10.5194/acp-2020-597
Preprint. Discussion started: 14 July 2020

Figure Captions

Figure 1 WRF-Chem simulation domain with topography. The blue circles represent centers of cities with ambient monitoring sites, and the size of circles denotes the number of ambient monitoring sites of cities. The red circle denotes observation site for aerosol species at the National Center for Nanoscience and Technology (NCNST), Chinese Academy of Sciences, Beijing.

Figure 2 Conceptual scheme of source apportionment for sulfate aerosols formed from (a) homogenous and (b) heterogeneous reactions. *FR*: formation rate; Superscript *i*: source number; Superscript *T*: total; Subscript *g*: gas phase; Subscript *a*: aerosol phase.

Figure 3 Conceptual scheme of source apportionment for nitrate and ammonium aerosols. Superscript *i*: source number; Superscript *T*: total; Subscript *g*: gas phase; Subscript *a*: aerosol phase.

Figure 4 Conceptual scheme of source apportionment for organic aerosols formed from (a) homogenous and (b) heterogeneous reactions. Superscript *i*: source number; Superscript *T*: total; Subscripts *j* and *k*: volatility bin number; Subscript *g*: gas phase; Subscript *a*: aerosol phase. AVOC/BVOC: VOCs emitted from anthropogenic/biogenic source; ASVOC/BSVOC: SVOC from oxidation of AVOC/BVOC; OPOG: oxidized POG. PSOA: SOA from oxidation and partitioning of POA treated as semi-volatile; ASOA/BSOA: SOA from oxidation of anthropogenic/biogenic VOCs; HSOA: SOA from irreversible uptake of glyoxal and methylglyoxal on aerosol/cloud surfaces.

Figure 5 Comparison of observed (black dots) and simulated (solid red lines) diurnal profiles of near-surface hourly mass concentrations of (a) $PM_{2.5}$, (b) O_3, (c) NO_2, (d) SO_2, and (d) CO averaged at monitoring sites in the NCP from 05 December 2015 to 04 January 2016.

Figure 6 Pattern comparisons of simulated (color counters) vs. observed (colored circles) near-surface mass concentrations of (a) $PM_{2.5}$, (b) O_3, (c) NO_2, and (d) SO_2 averaged from 05 December 2015 to 04 January 2016. The black arrows indicate simulated near-surface winds.

Figure 7 Comparison of measured (black dots) and simulated (black line) diurnal profiles of submicron aerosol species of (a) POA, (b) SOA, (c) sulfate, (d) nitrate, and (e) ammonium at NCNST site in Beijing from 05 December 2015 to 04 January 2016.

Figure 8 Spatial distribution of average $PM_{2.5}$ contributions from (a) Beijing, (b) Tianjin, (c) Hebei, (d) Shandong, (e) Henan, and (f) Shanxi provinces from 05 December 2015 to 04 January 2016.

Figure 9 Average $PM_{2.5}$ contributions (%) in (a) Beijing, (b) Tianjin, (c) Hebei, (d) Henan, (e) Shandong, and (f) Shanxi from local (red) and non-local (blue) emissions from 05 December 2015 to 04 January 2016 under different pollution levels.

Figure 10 Average aerosol constituent contributions (%) in (a) Beijing, (b) Tianjin, (c) Hebei, (d) Henan, (e) Shandong, and (f) Shanxi from local (red) and non-local (blue) emissions from 05 December 2015 to 04 January 2016.

https://doi.org/10.5194/acp-2020-597
Preprint. Discussion started: 14 July 2020

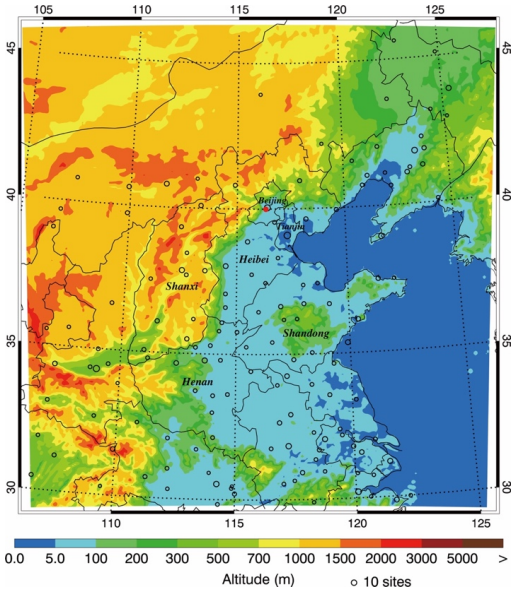

Figure 1 WRF-Chem simulation domain with topography. The circles represent centers of cities with ambient monitoring sites, and the size of blue circles denotes the number of ambient monitoring sites of cities. The red circle denotes observation site for aerosol species at the National Center for Nanoscience and Technology (NCNST), Chinese Academy of Sciences, Beijing.

https://doi.org/10.5194/acp-2020-597
Preprint. Discussion started: 14 July 2020

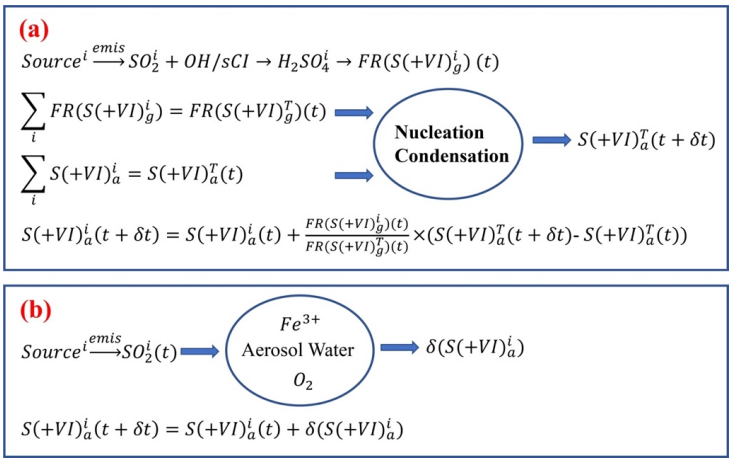

Figure 2 Conceptual scheme of source apportionment for sulfate aerosols formed from (a) homogenous and (b) heterogeneous reactions. *FR*: formation rate; Superscript *i*: source number; Superscript *T*: total; Subscript *g*: gas phase; Subscript *a*: aerosol phase.

https://doi.org/10.5194/acp-2020-597
Preprint. Discussion started: 14 July 2020

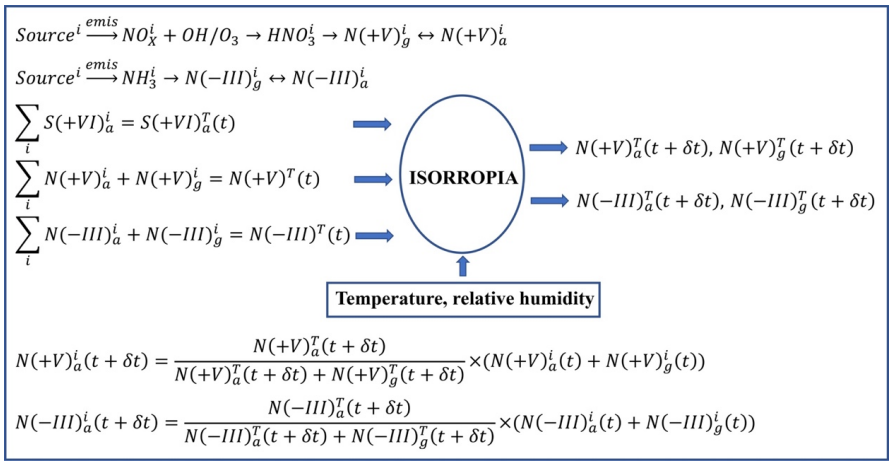

Figure 3 Conceptual scheme of source apportionment for nitrate and ammonium aerosols. Superscript *i*: source number; Superscript *T*: total; Subscript *g*: gas phase; Subscript *a*: aerosol phase.

https://doi.org/10.5194/acp-2020-597
Preprint. Discussion started: 14 July 2020

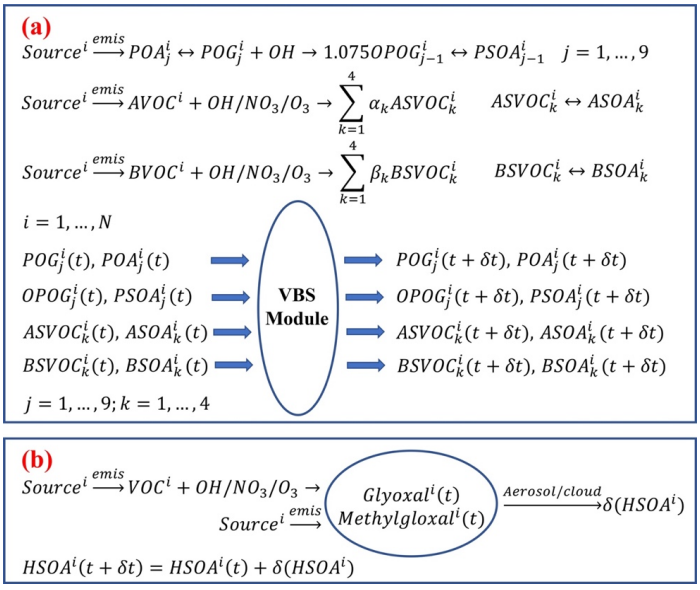

Figure 4 Conceptual scheme of source apportionment for organic aerosols formed from (a) homogenous and (b) heterogeneous reactions. Superscript *i*: source number; Superscript *T*: total; Subscripts *j* and *k*: volatility bin number; Subscript *g*: gas phase; Subscript *a*: aerosol phase. AVOC/BVOC: VOCs emitted from anthropogenic/biogenic source; ASVOC/BSVOC: SVOC from oxidation of AVOC/BVOC; OPOG: oxidized POG. PSOA: SOA from oxidation and partitioning of POA treated as semi-volatile; ASOA/BSOA: SOA from oxidation of anthropogenic/biogenic VOCs; HSOA: SOA from irreversible uptake of glyoxal and methylglyoxal on aerosol/cloud surfaces.

https://doi.org/10.5194/acp-2020-597
Preprint. Discussion started: 14 July 2020

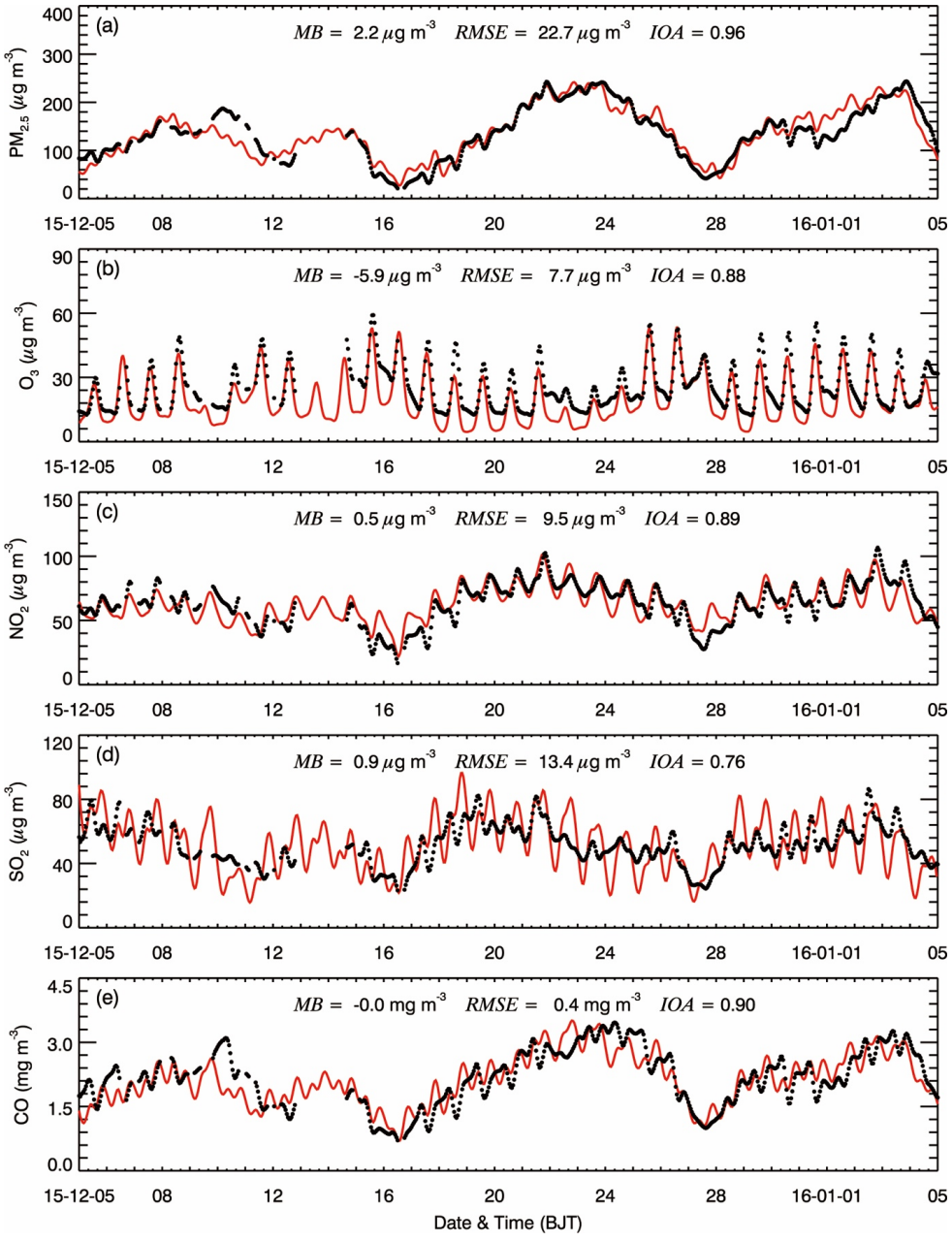

Figure 5 Comparison of observed (black dots) and simulated (solid red lines) diurnal profiles of near-surface hourly mass concentrations of (a) $PM_{2.5}$, (b) O_3, (c) NO_2, (d) SO_2, and (d) CO averaged at monitoring sites in the NCP from 05 December 2015 to 04 January 2016.

https://doi.org/10.5194/acp-2020-597
Preprint. Discussion started: 14 July 2020

Atmospheric Chemistry and Physics Discussions

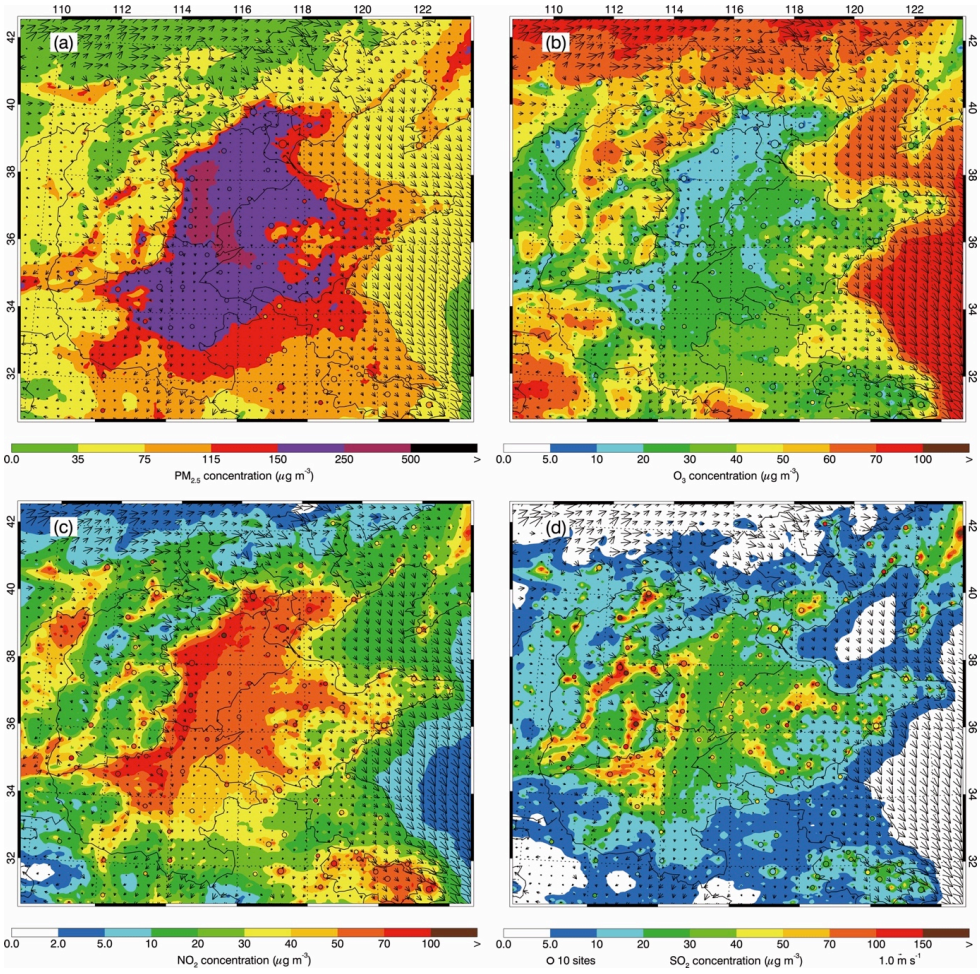

Figure 6 Pattern comparisons of simulated (color counters) vs. observed (colored circles) near-surface mass concentrations of (a) $PM_{2.5}$, (b) O_3, (c) NO_2, and (d) SO_2 averaged from 05 December 2015 to 04 January 2016. The black arrows indicate simulated surface winds.

https://doi.org/10.5194/acp-2020-597
Preprint. Discussion started: 14 July 2020

Atmospheric Chemistry and Physics
Discussions

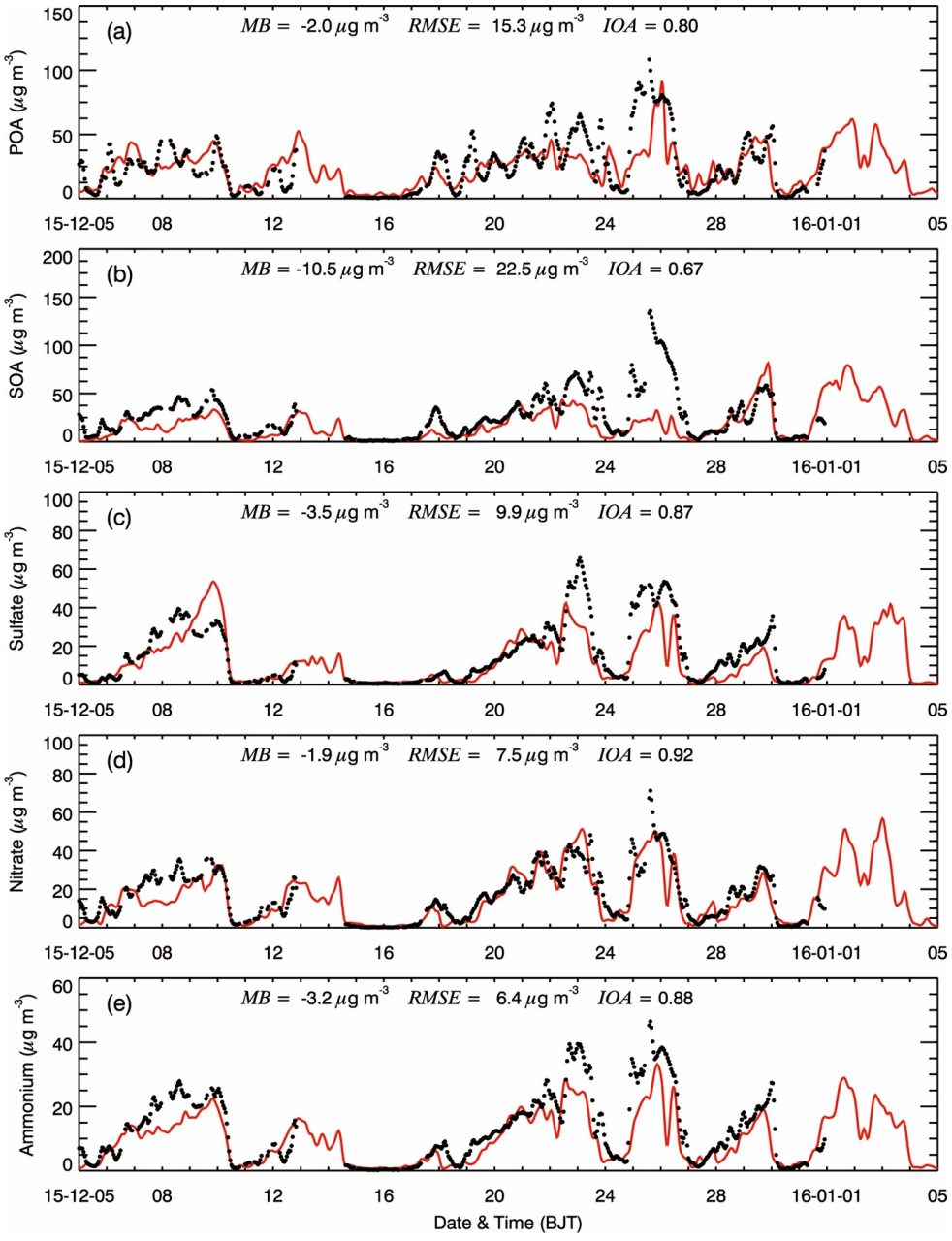

Figure 7 Comparison of measured (black dots) and simulated (black line) diurnal profiles of submicron aerosol species of (a) POA, (b) SOA, (c) sulfate, (d) nitrate, and (e) ammonium at NCNST site in Beijing from 05 December 2015 to 04 January 2016.

https://doi.org/10.5194/acp-2020-597
Preprint. Discussion started: 14 July 2020

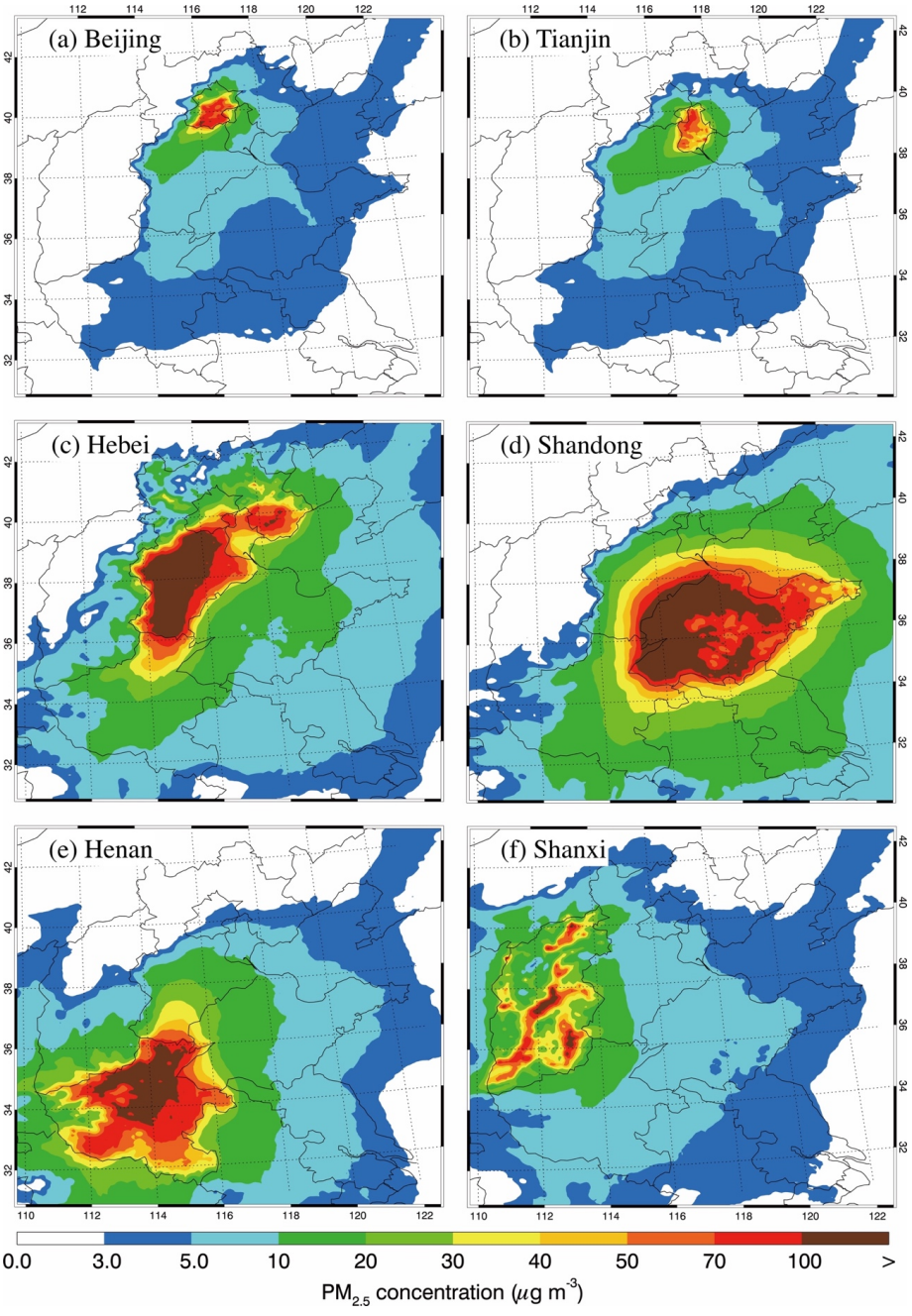

Figure 8 Spatial distribution of average $PM_{2.5}$ contributions from (a) Beijing, (b) Tianjin, (c) Hebei, (d) Shandong, (e) Henan, and (f) Shanxi provinces from 05 December 2015 to 04 January 2016.

https://doi.org/10.5194/acp-2020-597
Preprint. Discussion started: 14 July 2020

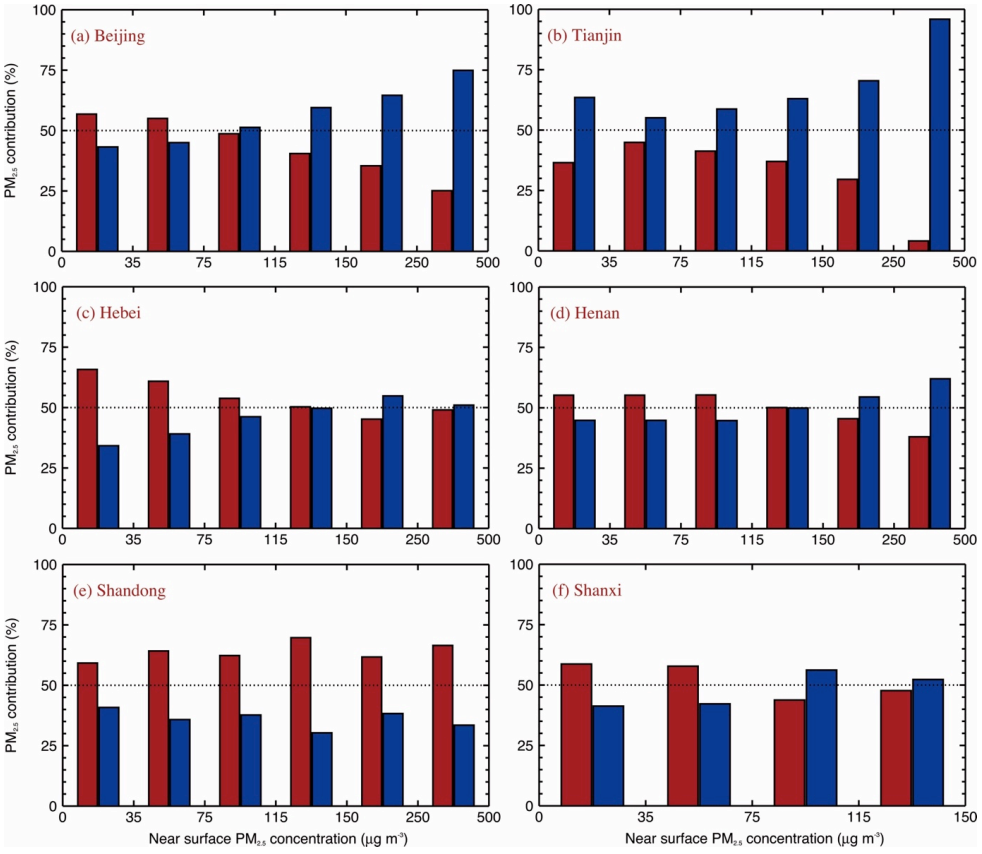

Figure 9 Average $PM_{2.5}$ contributions (%) in (a) Beijing, (b) Tianjin, (c) Hebei, (d) Henan, (e) Shandong, and (f) Shanxi from local (red) and non-local (blue) emissions from 05 December 2015 to 04 January 2016 under different pollution levels.

https://doi.org/10.5194/acp-2020-597
Preprint. Discussion started: 14 July 2020

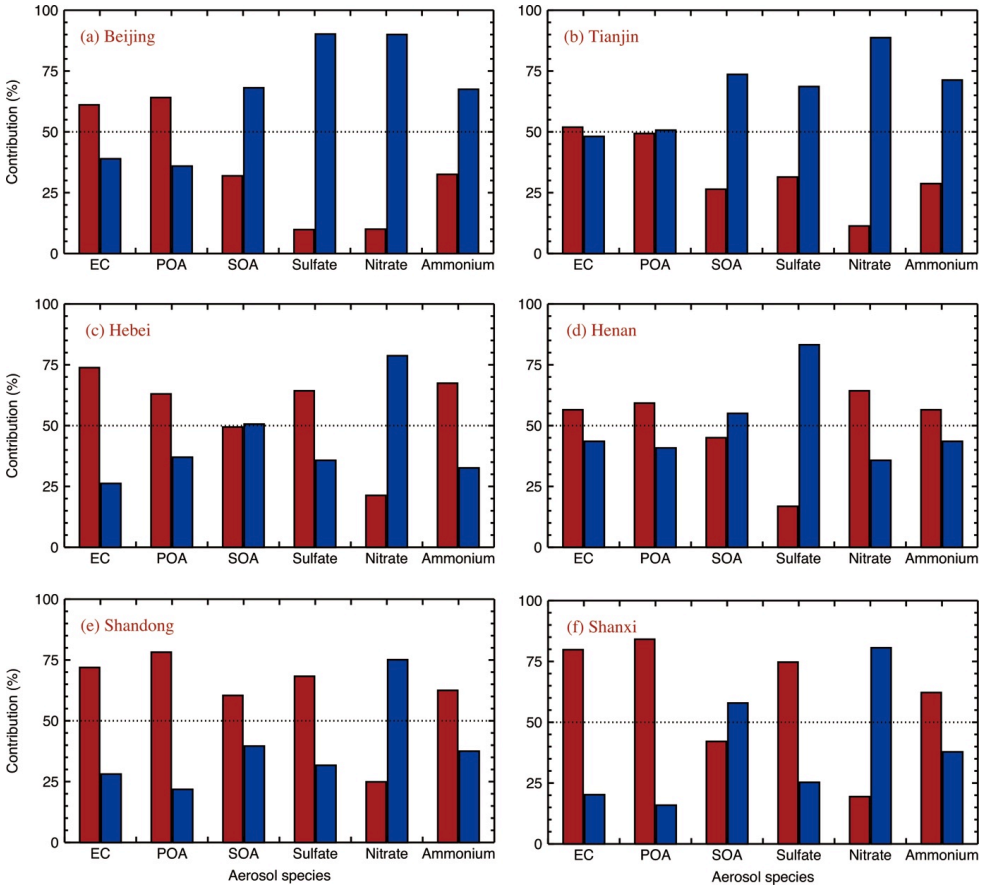

Figure 10 Average aerosol constituent contributions (%) in (a) Beijing, (b) Tianjin, (c) Hebei, (d) Henan, (e) Shandong, and (f) Shanxi from local (red) and non-local (blue) emissions from 05 December 2015 to 04 January 2016.